THE JOURNAL OF PHYSICAL CHEMISTRY B

Article

pubs.acs.org/JPCB

Both Zundel and Eigen Isomers Contribute to the IR Spectrum of the Gas-Phase $H_9O_4^+$ Cluster

Waldemar Kulig and Noam Agmon*

The Fritz Haber Research Center, Institute of Chemistry, The Hebrew University of Jerusalem, Jerusalem 91904, Israel

Supporting Information

ABSTRACT: The "Eigen cation", $H_3O^+(H_2O)_3$, is the most prevalent protonated water structure in the liquid phase and the most stable gas-phase isomer of the $H^+(H_2O)_4$ cluster. Nevertheless, its 50 K argon predissociation vibrational spectrum contains unexplainable low frequency peak(s). We have simulated the IR spectra of 10 gas-phase $H^+(H_2O)_4$ isomers, that include zero to three argon ligands, using dipole autocorrelation functions from ab initio molecular dynamics with the CP2K software. We have also tested the effect of elevated temperature and dispersion correction. The Eigen isomers describe well the high frequency portion of the spectrum but do not agree with experiment below 2000 cm^{-1}. Most notably, they completely lack the "proton transfer bands" observed at 1050 and 1750 cm^{-1}, which characterize Zundel-type ($H_5O_2^+$) isomers. In contrast, linear isomers with a Zundel core, although not the lowest in energy, show very good agreement with experiment, particularly at low frequencies. Peak assignments made with partial velocity autocorrelation functions verify that the 1750 cm^{-1} band does not originate with the Eigen isomer but is rather due to coupled proton transfer/water bend in the Zundel isomer.

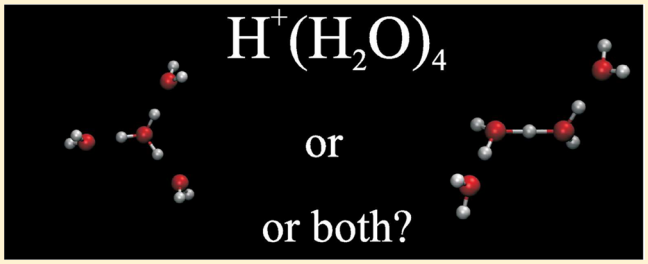

INTRODUCTION

The protonated water tetramer, $H_9O_4^+$, assumes a central role in aqueous acidic solutions, since Eigen and collaborators[1] have suggested that its $H_3O^+(H_2O)_3$ isomer, the triply hydrated hydronium, is the dominant form there. Earlier, Huggins proposed that the proton bridges two water molecules,[2] forming a protonated water dimer, $H_5O_2^+$. It was Zundel who popularized this moiety,[3] nowadays known as the "Zundel cation", arguing that it gives rise to a "continuum" in the infrared (IR) absorption from aqueous acidic solutions. There has been a prolonged debate[4,5] on whether the Eigen (E) or Zundel (Z) cations represent the correct structure of protonated liquid water. In modern mechanisms of proton mobility in water,[6] the more stable (yet distorted) E-cation converts, through a Z-intermediate, to an analogous E-cation centered on a neighboring water molecule. This E-Z-E scenario was corroborated by molecular simulations.[7−9]

In the liquid phase, it is difficult to isolate the IR signal from these two limiting structures.[10−12] Consequently, the past decade has witnessed intensified efforts directed toward isolating and recording the IR spectra of protonated water clusters, $H^+(H_2O)_n$, in the gas phase.[13−25] Since the early measurements of the $H^+(H_2O)_4$ vibrational spectrum,[13] this cluster was assumed to possess the symmetric E-structure: "The n = 4 complex is expected to be the classic Eigen ion, having a central hydronium surrounded symmetrically by three water molecules each hydrogen bonded to a single OH".[21] It "has a minimum energy structure well described as an H_3O^+ Eigen core, symmetrically solvated by three dangling water molecules".[19] Consequently, "it has been known that $H^+(H_2O)_4$ has the form of the symmetrically hydrated H_3O^+ core and is called Eigen cation. No other isomers have been observed".[23] Indeed, it is widely believed that $H^+(H_2O)_6$ is the smallest cluster for which multiple isomers can coexist.[15,23,25]

Isomeric structures of $H^+(H_2O)_4$ are shown in Figure 1. Indeed, the most stable one is the symmetric E-cluster (C_3 symmetry).[15,21,26,27] However, lying only 2.3 kcal/mol above it (zero point energy included) is the cis-Z isomer (C_2 symmetry).[21,26,27] MP2(TZ2P) calculations have shown[26] that it differs from the E-isomer in the low energy part of the spectrum (below 2000 cm^{-1}), where the Z-cluster has several strong peaks while the E-cluster has extremely weak features. This observation went unnoticed, because the early measurements[13−15] (and even some recent ones[21,23]) were limited to the high frequency region, above 2000 cm^{-1}. Recently, however, the argon-predissociation vibrational spectrum of the $H^+(H_2O)_4$ cluster was measured (at 50 K) in both the high and low frequency regimes.[19,22] These experiments do show noticeable low frequency bands, yet the observed spectrum was unanimously assigned to the E-cation.

Theory can be indispensable in identifying the absorbing isomer. For the protonated dimer (n = 2), high level quantum calculations using the multi configuration time dependent Hartree (MCTDH) method[28,29] show excellent agreement

Received: October 22, 2013
Revised: December 17, 2013
Published: December 17, 2013

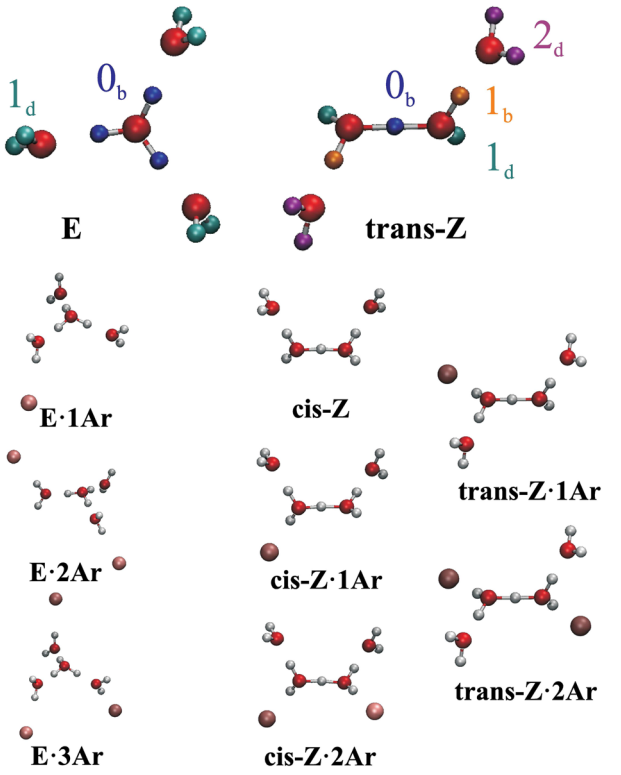

Figure 1. The geometry of the initial conformations chosen for the 10 simulated protonated water tetramer systems. These conformations were optimized in Gaussian 03,[30] with their *XYZ* coordinates given in the Supporting Information. The figure also defines the (colored) proton classes of the *E* and *Z* isomers, which are denoted by 0_b, 1_b, 1_d, and 2_d. The numerals denote the solvation shell of the excess proton, whereas the indices stand for d = dangling (not hydrogen-bonded) and b = (hydrogen) bonded. Argon atoms are rendered in pink.

with experiment.[20] This method cannot presently be extended to larger clusters, for which it is common to use quantum chemistry packages, such as Gaussian 03,[30] for calculating IR spectra. Although anharmonic frequencies can be calculated in this method,[31] usually only harmonic frequencies are utilized in the analysis. Here (quadratic) force constants are calculated near the minimum of the potential energy. The normal-mode matrix is then diagonalized to generate the vibrational frequencies. Such IR spectra are shown in our Supporting Information. The drawbacks of this static method are that it (a) samples only configurations near the minimum of the potential and (b) utilizes harmonic force constants.

An alternative, dynamic calculation of IR spectra from molecular trajectories utilizes the Fourier transform of the dipole−dipole autocorrelation function (DACF). This samples all the configurations from a classical trajectory (not only the potential minimum), and hence does not assume harmonicity. To obtain spectroscopic accuracy, trajectories are calculated using various flavors of ab initio molecular dynamics (AIMD),[12,31−40] in which the forces are computed every time step from density functional theory (DFT).[41] For protonated water clusters, most of such calculations have focused on H_3O^+,[39,40] and on $H_5O_2^+$.[32−34,36,37,39] The more recent calculations[37,39] show that AIMD can generate the IR spectrum of the protonated water dimer with a quality approaching that of MCTDH. This motivates the use of AIMD methods for analyzing the spectra of the larger clusters.

Park et al.[31] have performed Car−Parrinello AIMD on the *E*-isomer, noting that the experimentally observed peak near 1760 cm^{-1} is missing in their simulated spectrum, and that this peak has been previously identified in the Zundel cluster and assigned to the terminal water bends[17] and/or their combination with the shared proton motion.[18] This vibrational mode has quite an important role in proton mobility, as it has also been identified as the "proton transfer mode" (PTM) for aqueous acid solutions.[12] Nevertheless, a systematic study of higher energy isomers that might account for the missing peaks has not yet been attempted. This is the goal of the present work.

Here we perform AIMD simulations using the CP2K package,[42] from which we calculate the IR spectra of the 10 $H^+(H_2O)_4$ structures shown in Figure 1. These consist of the *E*, cis-*Z*, and trans-*Z* isomers with zero to three Ar atoms. We have also checked the effect of temperature and dispersion correction (DC) on these spectra. We find that the spectra of the *E*-isomers (without or with Ar) indeed do not agree with experiment in the low frequency regime, whereas the trans-*Z* isomers show near-quantitative agreement.

METHODS

a. Static Spectra. As a reference, we have first calculated the static spectra obtained in the harmonic approximation using quantum chemistry methods for the 10 $H_9O_4^+ \cdot n$Ar clusters (n = 0−3) in Figure 1. We have used a DFT method (B3LYP functional with the aug-cc-pVTZ basis set in Gaussian 03),[30] which could be more meaningfully compared with the dynamic DFT spectra from CP2K below. The corresponding coordinates and IR spectra are collected in the Supporting Information.

While the harmonic IR spectrum for the *E*-cation using the B3LYP functional has been presented before,[23] it is more common to perform the calculation on the MP2 level.[19,21,26] MP2 typically gives better structures and energies, but B3LYP gives better harmonic IR frequencies. This is corroborated in Figure 2 for the dominant peak of the *E*-cation. However, an *anharmonic* MP2/aug-cc-pVDZ calculation can reproduce this band most accurately.[31]

When considering the high frequency regime, harmonic MP2 frequencies were scaled empirically by a factor of about 0.95.[19,21,31] However, at low frequencies, harmonic frequencies *underestimate* the experimental ones. For example, for $H_5O_2^+$, the shared proton band that occurs experimentally[20] at 1047 cm^{-1} is found by MP2/aug-cc-pVTZ at 884 cm^{-1},[33] by B3LYP/aug-cc-pVTZ at 926 cm^{-1},[12] and by AIMD with the BLYP/DZVP functional at 1031 cm^{-1}.[12] Because we need to consider here both high and low frequencies, a uniform scaling of harmonic frequencies is not practical.

Experimental groups tend to focus on the high frequency region of the spectrum (free OH, above 3500 cm^{-1}), counting the number of unique OH stretching modes and basing their assignment on that. The Gaussian 03 spectra in the Supporting Information show that, for all isomers considered here, two distinguishable peaks are obtained at about the same frequencies. Hence, in this case, the high end of the spectrum cannot be utilized to differentiate between isomers.

b. Dynamic Spectra. We performed AIMD simulations of H_3O^+ and the 10 $H_9O_4^+ \cdot Ar_n$ clusters (n = 0−3) in Figure 1 using the CP2K/Quickstep software package;[42] see http://cp2k.berlios.de. This involves classical nuclear dynamics with forces obtained every time step by solving the Schrödinger

dx.doi.org/10.1021/jp410446d | J. Phys. Chem. B 2014, 118, 278−286

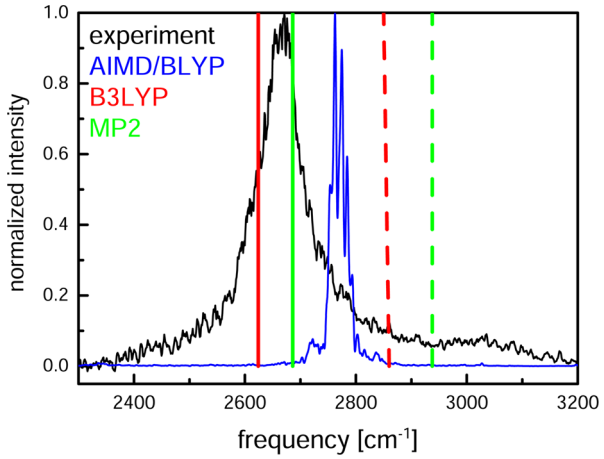

Figure 2. The dominant peak of the $H^+(H_2O)_4$ cluster, comparing experiment (black line)[19] with harmonic (dashed lines) and anharmonic (full lines) quantum chemistry calculations for the *E*-isomer. Green: MP2/aug-cc-pVDZ (harmonic from p S24 of the Supporting Information of ref 21, anharmonic from Table 4 of ref 31). Red: B3LYP/aug-cc-pVTZ, this work. Blue, our dynamic AIMD calculations.

equation for the electrons using DFT with a mixed Gaussian and plane-wave approach. The BLYP functional with the double-ζ valence polarization (DZVP) basis set and Goedecker–Teter–Hutter pseudopotentials were used.[43] The plane-wave energy cutoff was set to 300 Ry. Self-interaction correction (SIC) was applied with the Martyna–Tuckerman Poisson equation solver.[44] These conditions are similar to those in recent simulations of $H_3O^+(H_2)_n$ clusters (n = 0–3).[40] To obtain DC for the clusters containing the polarizable Ar atom, *E*·1Ar and *Z*·1Ar, we have repeated these calculations with the BLYP-D3 functional[45] and the same basis set.

The geometry of each starting structure was taken from the Gaussian 03 calculations described above. Their accuracy is not a concern here, because these structures were subsequently equilibrated in CP2K for at least 5 ps in the canonical (NVT) ensemble. The target temperature was 50 K, maintained by a Nosé–Hoover thermostat (of chain length 3). A few simulations with T = 150 K were also conducted in order to sample higher energy regions in the anharmonic potential.

After equilibration, each trajectory was continued for 20 ps (the *E*, trans-*Z*, and trans-*Z*·2Ar clusters) or 10 ps (all other clusters) in the microcanonical (NVE) ensemble with a time step of 0.5 fs. Coordinates and velocities were saved every time step, to ensure that the spectra at high frequencies are not corrupted.

The relatively large time step of 0.5 fs, which allows running longer trajectories, is enabled by setting hydrogen masses to 2 u.[46] This requires subsequent scaling of all OH frequencies by the square root of the OD/OH reduced mass ratio (i.e., all OH frequencies were scaled, whereas OO frequencies were not). The scaling factor is thus $(2 \times 17/18)^{1/2}$ = 1.37, and this matches the sharp water bending band at 1615 cm^{-1}.[12]

The actual trajectories can be visualized by running the movie files in the Supporting Information. Movie S0 shows the trajectory of the trans-*Z* conformer as outputted from CP2K. Slight drift in the center of mass and orientation is visible, likely due to limitations in energy conservation (the energy drift in our simulations increases roughly linearly in time at a pace of 0.1 kcal/mol per 10 ps). The remaining movies S1–S8 show the trajectories of the *E*- and trans-*Z* isomers after realigning the center of mass in each frame to eliminate the drift. These demonstrate that during the simulations the topology of the studied isomers does not change.

The IR absorption coefficient, $\alpha(\omega)$, was computed from the autocorrelation function (ACF) of the system's dipole moment

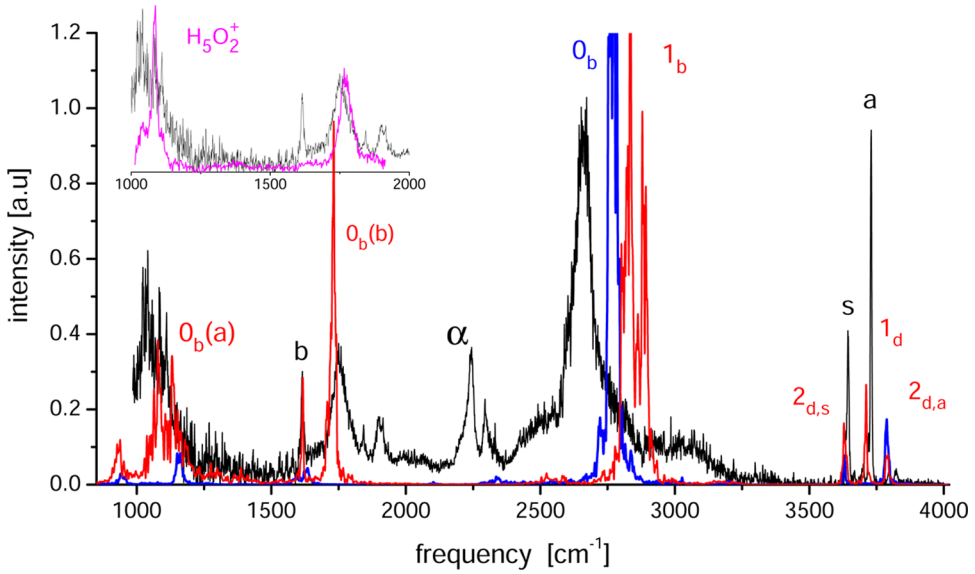

Figure 3. Comparison of the Ar-tagged photodissociation spectrum of the gas-phase $H_9O_4^+$ cluster (Figure 5c of ref 22, courtesy of Mark A. Johnson), black line, with our AIMD spectra (20 ps trajectory) of the *E*- and trans-*Z* isomers (blue and red lines, respectively). The experimentally assigned symmetric stretch, asymmetric stretch, and bending vibrations of free water hydrogens are denoted by **s**, **a**, and **b**, respectively. Also indicated is the α-band.[24] Calculated OH-stretch bands of hydrogen-bonded hydrogens originate from proton types 0_b for the *E*-isomer or 0_b and 1_b for the *Z*-isomer (see Figure 1 for notations). The inset compares the same experimental spectrum (black line) with that[19] of $H_5O_2^+$ (magenta) below 2000 cm^{-1}. Note that the high frequency OH region is displayed in Figure 7 below.

dx.doi.org/10.1021/jp410446d | J. Phys. Chem. B 2014, 118, 278–286

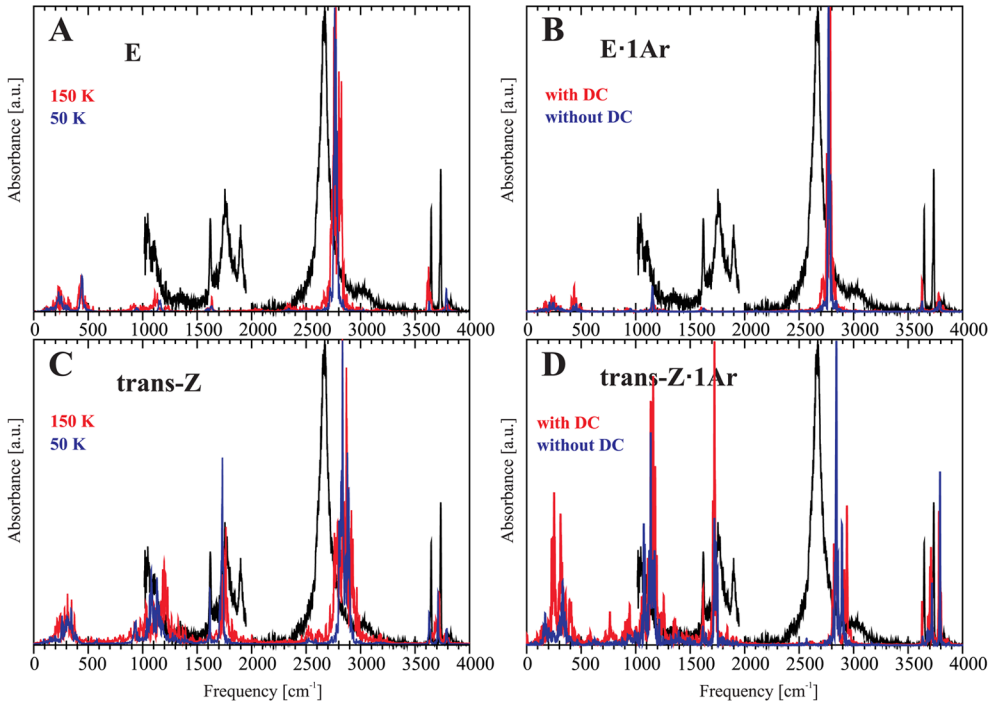

Figure 4. Temperature and DC dependence of the AIMD IR spectra for the *E*- and *Z*-isomers of the $H^+(H_2O)_4$ cluster: (A) the *E*-isomer at 50 and 150 K with no DC; (B) the *E*·1Ar isomer at 50 K with and without DC; (C) the trans-*Z* isomer at 50 and 150 K with no DC; and (D) the trans-*Z* isomer at 50 K with and without DC. Black lines are the experimental spectra at 50 K from ref 19, which correspond to clusters tagged with 1Ar. No DC = BLYP functional, whereas DC = BLYP-D3 functional in CP2K. The 50 K no DC results, from 20 ps trajectories, are identical to those in Figures S6, S25, and S31 in the Supporting Information, whereas the 150 K and DC spectra are from 10 ps trajectories that do not appear in the Supporting Information.

time derivative $\langle \dot{\boldsymbol{\mu}}(0)\dot{\boldsymbol{\mu}}(t)\rangle$ (DACF), by taking (the real part of) its temporal Fourier transform

$$\alpha(\omega) = A\Re \int_0^\infty dt e^{-i\omega t}\langle \dot{\boldsymbol{\mu}}(0)\dot{\boldsymbol{\mu}}(t)\rangle \quad (1)$$

Here $\omega = 2\pi\nu$, with ν being the vibrational frequency and A a normalization factor. This form, e.g., eq 10 in ref 35, includes a harmonic quantum correction to the classical ACF and a factor ω^2 arising from replacement of $\boldsymbol{\mu}(t)$ by its time derivative. The latter was obtained from the CP2K output and differentiated numerically. We have checked that using $\boldsymbol{\mu}(t)$ itself in calculating the ACF results in negligible changes to the spectrum. The index of refraction is approximately unity for gas-phase spectroscopy, and therefore, it does not appear in the above equation.

RESULTS

The central results of this work are the AIMD generated IR spectra of the *E* and *Z* isomers that are compared with the most recent experimental spectrum[22] in Figure 3.

a. The Experimental Spectrum. According to its accepted interpretation,[19] the sharp peaks denoted by **b**, **s**, and **a** originate from the "dangling" hydrogens of the outer water molecules. Their symmetric (**s**) and asymmetric (**a**) OH stretch frequencies occur at the blue edge of this spectrum, close to their location for an isolated water molecule, while the free water HOH bend (**b**) is the sharp peak at 1615 cm^{-1}.

All other features in the experimental spectrum must therefore originate from the hydrogen-bonded hydrogen atoms. The strong peak at 2665 cm^{-1} is due to their OH stretch. It is red-shifted by ca. 1000 cm^{-1} from the free OH stretch, because some of the covalent-bond electron density has shifted to the hydrogen bond. If the observed spectrum is attributed to the *E*-isomer,[13−16,19−24] then this peak must be assigned to the hydronium OH-stretching modes, predominantly to the asymmetric stretch of the H_3O^+ core.[19] The best theoretical agreement is obtained from an anharmonic MP2/aug-cc-pVDZ calculation,[31] 2686 cm^{-1}, supporting its conventional assignment to the *E*-isomer.

The peak at 1750 cm^{-1}, which is "markedly similar to that displayed by the isolated *Z*-ion"[19] (indeed see the inset of Figure 3), has more recently been assigned to the HOH bend in a H_3O^+ core.[24] Although in free H_3O^+ this band is found at 1622 cm^{-1} (see, for example, Figure S3 in the Supporting Information), it blue shifts to 1659 cm^{-1} in $H_3O^+(N_2)_3$. The "α band" at 2245 cm^{-1} was not seen in earlier experiments,[19] which are reproduced in Figure 4 here, likely because it occurs in a spectral region that is difficult to access experimentally. It was assigned to a combination of frustrated rotation plus bending of the hydronium core in the *E*-isomer.[24] Three weak features at 1847, 1904, and 2307 cm^{-1} are probably also combination bands that remain unassigned. Finally, there is an unassigned intense wide peak near 1050 cm^{-1}.

Let us now compare this spectrum with our theoretical AIMD simulations.

b. *E*-Isomer Spectra. The *E*-isomer (blue spectrum in Figure 3) exhibits a single strong peak at 2775 cm^{-1}, just 110 cm^{-1} blue-shifted from the experimental. In addition, there are some weak features in the background. To make these visible, we have overnormalized this main peak. Now one can see two bands in the high frequency end, with the dominant one somewhat blue-shifted from the experimental **a** band. In the low frequency regime, there is a remnant of the water bend **b**, and a weak narrow peak near 1150 cm^{-1} (probably the

dx.doi.org/10.1021/jp410446d | J. Phys. Chem. B 2014, 118, 278−286

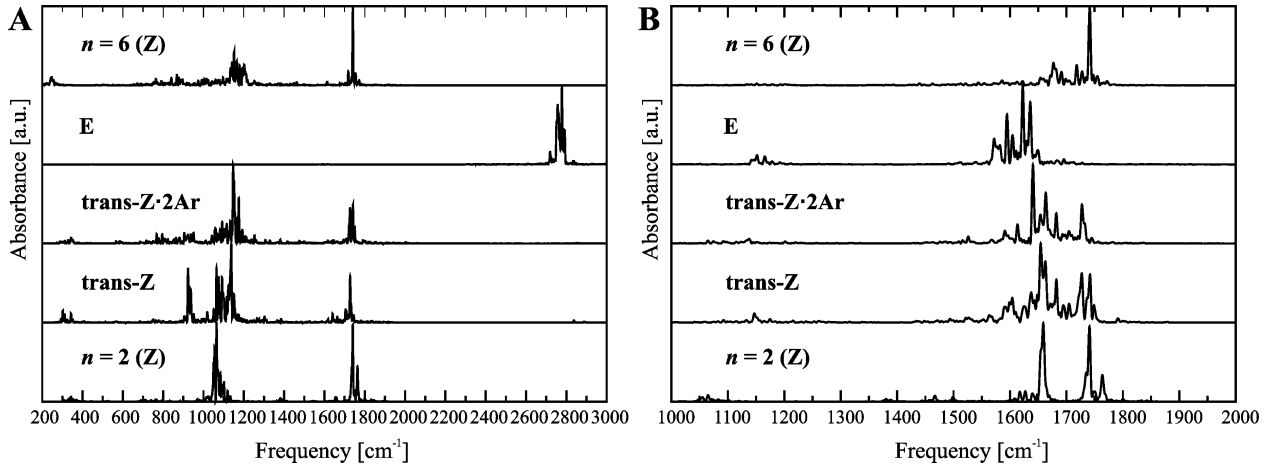

Figure 5. Partial VACF (A) stretching and (B) bending spectra from AIMD trajectories of $H^+(H_2O)_n$ gas-phase clusters. Stretching VACFs are for the proton(s) closest to the excess charge: one of the H_3O^+ protons for the *E*-cluster and H* in the $H_2OH^*OH_2$ moiety of the *Z*-clusters. Bending VACFs used the HOH angles of these two moieties. n = 4 present study; n = 2 and 6 uses data from ref 12.

hydronium core pyramidal motion), where experimentally there is a wide intense band. Most conspicuous is the complete absence of the 1750 cm^{-1} band, even when the spectrum is magnified to reveal near-background detail. In about 4 orders of magnitude of calculated intensities, we see no hint for this feature.

The absence of a 1750 cm^{-1} band is not unique to AIMD. It is shared by harmonic MP2(fc)/aug-cc-pVDZ (p S27 of the Supporting Information of ref 21), anharmonic MP2/aug-cc-pVDZ (Table 4 of ref 31), and our B3LYP/aug-cc-pVTZ calculations (Figure S5 in the Supporting Information). In addition, a recent AIMD calculation (with the PBE functional) for an *E*-isomer that is further solvated by one hydrogen and two water molecules (Figure 3F of ref 25) also lacks any absorption near 1750 cm^{-1}.

One may argue that the Ar atom attached to these clusters in the molecular beam could change the calculated spectrum appreciably. Therefore, we have also calculated the static (Gaussian 03) and dynamic (CP2K) spectra of the *E*-isomer with one, two, and three Ar atoms attached (see Figures S7–S15 in the Supporting Information). Ar attachment changes (mostly) the relative intensities of the bands and their shapes. Consequently, *E*·2Ar shows the best agreement with experiment (Figure S12 in the Supporting Information), with more intense free water **s**, **a**, and **b** bands. However, neither it nor the other two isomers show any signal at 1750 cm^{-1}.

Another concern may arise if the spectrum changes strongly with temperature (T), and unpopulated vibrational transitions become populated at higher T. This may be an issue because, in the absence of quantum nuclear dynamics, the simulated T may not correspond precisely to the experimental one. To check this issue, we have calculated the *E*-isomer spectrum also at 150 K (Figure 4A). It is seen that the main peak becomes wider, and there are slight variations in intensity. The effect of DC for the *E*·1Ar isomer is shown in Figure 4B, which is almost indistinguishable from the case without DC. Thus, temperature or dispersion effects do not alter our conclusion that an assignment in terms of the *E*-isomer alone cannot be correct. The monitored clusters must contain at least one additional isomer that does absorb near 1050 and 1750 cm^{-1}. The resemblance with the corresponding $H_5O_2^+$ peaks (inset of Figure 3) suggests that this may be a *Z*-isomer.

c. *Z*-Isomer Spectra. The cis-*Z* conformer is next in energetic order.[21,26,27] Its simulated AIMD spectrum (Figure S18 in the Supporting Information) indeed exhibits a small peak at 1740 cm^{-1}. However, when we added one or two Ar atoms to this cluster (Figures S19 and S21 in the Supporting Information), it converted to the trans-conformer already during the equilibration stage.

The trans-*Z* conformer (Figure 1) has rarely been considered.[47] It is stable toward the addition of one or two argon atoms, so we can compute the AIMD spectrum, which is shown in red in Figure 3. Its amplitude is normalized to the experimental water bending band (at 1615 cm^{-1}). Its main peak is somewhat blue-shifted as compared with the *E*-isomer (near 2835 cm^{-1}). Most notably, however, it does show an absorption band at 1732 cm^{-1}.

We have also computed its spectrum with one or two Ar atoms attached, using both static (Gaussian 03) and dynamic (CP2K) approaches (Figures S26–S31 in the Supporting Information). All of these spectra without exception (as well as all the cis-*Z* spectra, Figures S16–S22 in the Supporting Information) show the 1750 cm^{-1} band.

In addition, the *Z*-isomer shows a wide intense band (actually a doublet) centered around 1100 cm^{-1}. This agrees with the strong experimental peak near 1050 cm^{-1}, contrasting with the *E*-isomer that shows only a weak narrow band near 1150 cm^{-1}. Indeed, as the inset to Figure 3 shows, the two peaks at 1070 and 1770 cm^{-1} characterize the $H_5O_2^+$ cluster.[19] They derive their intensity from the shared proton motion in the *Z*-cation, and are clearly manifested in the spectrum of the protonated tetramer. In contrast, the *E*-isomer has no shared proton modes and thus no strong absorptions in this region.

Figure 4C shows that these spectral features are not fundamentally different at 150 K. Figure 4D shows that the addition of Ar further enhances these low frequency peaks, which become even more intense when DC is included. The band around 2800–3000 cm^{-1} is then no longer dominant, suggesting perhaps that the main peak in the observed spectrum is due to the *E*-isomer, whereas the *Z*-isomer contributes to its blue shoulder.

Missing from our spectra of both *E*- and *Z*-isomers is the α-band at 2245 cm^{-1}, and the three other weak combination bands (at 1847, 1904, and 2307 cm^{-1}). These combination bands may perhaps be observed by AIMD only under specific

dx.doi.org/10.1021/jp410446d | J. Phys. Chem. B 2014, 118, 278–286

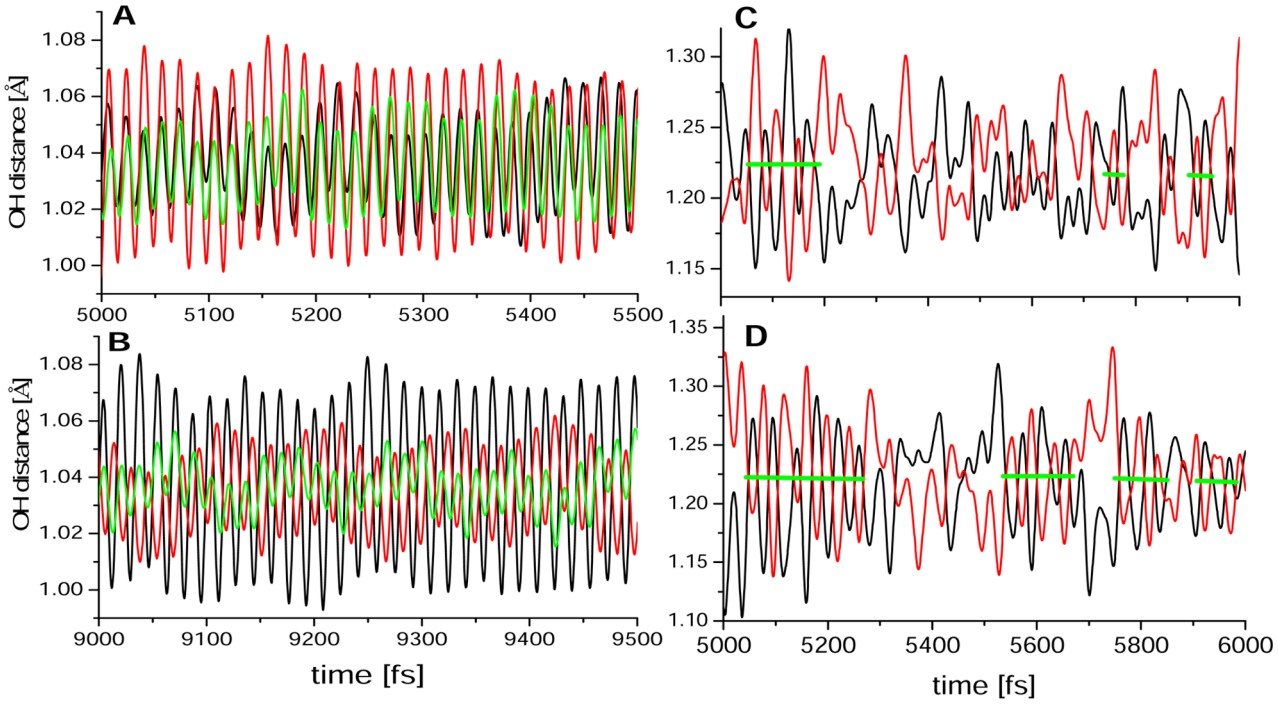

Figure 6. Time dependencies of the OH distances near the protonated cores of the *E* and *Z* clusters from 50 K AIMD trajectories. (A) The three OH distances of the H_3O^+ core in a time window in which all three are in-phase. (B) A time window in which two OH distances are in-phase (green and black) and the third in antiphase. There are also time windows (not shown) in which no two OH bonds vibrate in phase. (C) The two OH* distances in the OH*O moiety of the trans-*Z* isomer without Ar ligands, and (D) with two Ar ligands. Green line segments denote epochs of "regular vibration", where the plots of the two oscillating OH distances intersect during at least two consecutive oscillations. Clearly, the addition of Ar ligands renders the oscillatory motion more regular, and this may explain the more intense 0_b bands in Figure 4 above.

conditions, because for $H_5O_2^+$ the combination band found by MCTDH at 918 cm^{-1},[28] and experimentally at 928 cm^{-1},[20] was obtained by the AIMD simulations of Kaledin et al. at 30 K but not at 1, 50, or 80 K.[37] Perhaps there is a specific temperature at which our simulations will show the above-mentioned combination bands, but more likely this may require considerably longer trajectories. Although we do not observe the α-band directly, we do see a strong shared-proton band around 1100 cm^{-1}, and the α-band may simply be its first overtone.

d. Partial VACF Assignments. To aid in peak assignments using a simplified analysis of the vibrational bands, one may replace $\dot{\boldsymbol{\mu}}(t)$ in eq 1 by velocities, $\dot{\boldsymbol{R}}(t)$, thus obtaining the velocity autocorrelation function (VACF). Partial VACFs, which involve the velocities of single atoms or a group of atoms, have been used successfully in IR peak assignments.[48,49] For example, the partial VACF of the shared proton, H*, in a Zundel moiety will give us a precise indication as to where this proton absorbs. In the same vein, one may compute the partial angular VACF of three adjacent atoms to locate their bending signal.

Figure 5 shows the Fourier transform of the partial VACF for (A) the OH distance and (B) the HOH angle, of the OH and HOH moieties closest to the protonated core. Thus, we can see where these (local) modes are active. The hydronium OH stretch of the *E*-isomer is active only near 2775 cm^{-1}, in agreement with the DACF spectrum in Figure 3. In agreement with the bending frequency of the bare hydronium (Figure S3 in the Supporting Information), the VACF for the hydronium HOH angle in the *E*-isomer is active near 1615 cm^{-1}, and below (Figure 5B), but *not* near 1750 cm^{-1}, as suggested in ref 24. The 1750 cm^{-1} band is therefore not a hydronium band. A weak band near 1150 cm^{-1} appears both in the bending VACF and DACF, which might therefore be due to hydronium pyramidal motion.

For the *Z*-isomers, Figure 5A shows the partial VACF spectra for H* vibration in $H^+(H_2O)_n$ clusters with n = 4 (present work) as compared to the n = 2 and 6 clusters from ref 12. The 1050 and 1750 cm^{-1} bands are observed here for all *Z*-isomers, implying that *both* bands originate from[12] (or bear contributions from)[28] the excess proton. We thus denote them by 0_b(a) and 0_b(b) in Figure 3.

The 1750 cm^{-1} band is coupled to water bending in the $H_2O\cdots H^*\cdots OH_2$ unit of the *Z*-isomers, as seen in the bending VACF spectrum in Figure 5B, which exhibits a band at the same frequency. Peaks are sharpest for $H_5O_2^+$, where the (IR active) *ungerade* (1740 cm^{-1}) and (IR inactive) *gerade* (1656 cm^{-1}) modes correspond to out-of-phase and in-phase water bending, respectively. A full dimensional quantum dynamical simulation of $H_5O_2^+$ finds them at 1741 and 1606 cm^{-1}, respectively (Table 1 of ref 28). This corroborates our calculation and shows that the PTM is coupled to the *ungerade* bending mode.[28,37]

The involvement of (at least) two frequencies in the H* vibration can be seen by comparing the time dependencies of the OH distances in the protonated cores of the *E*- and trans-*Z* isomers (Figure 6). For the H_3O^+ core of the *E*-isomer (panels A, B), the three distances are on average equal (and small), while for the OH*O core of the *Z*-isomer (panels C, D) the two distances are roughly equal (and large). While in panels A and B we see regular vibration with a single (high) frequency, the H* vibration in panels C and D clearly involves a superposition of several frequencies, as identified by its partial VACF in Figure 5A.

dx.doi.org/10.1021/jp410446d | J. Phys. Chem. B 2014, 118, 278−286

Figure 7 shows the partial VACF for protons (other than H*) of the trans-*Z* isomers in the high frequency regime. The hydrogen-bonded 1_b protons give rise to the main peak at 2856 cm^{-1}. The OH stretching bands of dangling protons occur above 3600 cm^{-1}. Experimentalists attribute the two strong bands in this region to the **s** and **a** modes of the outer water molecules. The AIMD results of the trans-*Z* isomer might suggest an alternative picture. Its 1_d signal is always in between the symmetric and asymmetric stretch of the free water in the second solvation shell ($2_{d,s}$ and $2_{d,a}$, respectively). The two strong peaks thus originate from two different water molecules, one from the second shell ($2_{d,s}$), at the lower frequency, and a second from the first shell (1_d), at the higher frequency. A third, much weaker, peak (that is also seen experimentally) arises from the asymmetric stretch of the outer water molecules, $2_{d,a}$. However, we are not advocating this as an assignment to the observed spectrum, because the present calculations do not have sufficient accuracy to account for close-lying peaks and their relative intensities. For example, the relative intensities of the $2_{d,s}$ and $2_{d,a}$ peaks (e.g., in panels A and B) are quite sensitive to perturbations such as adding Ar atoms.

DISCUSSION AND CONCLUSIONS

The Eigen cation is a key for understanding protonated water in the liquid phase. In the gas phase, it is the lowest energy isomer of the $H^+(H_2O)_4$ cluster. Therefore, it was natural to expect that the experimentally recorded predissociation IR spectrum corresponds to this symmetrically solvated hydronium, $H_3O^+(H_2O)_3$ or *E*-isomer. Most of the earlier IR spectroscopy of protonated water clusters accessed only the high-frequency regime, above 2000 cm^{-1}. Here good agreement was found between the theoretical spectrum of the *E*-isomer and experiment. The seminal work of Headrick et al.[19] reported spectral features below 2000 cm^{-1}, which were corroborated in later experimental work.[22] Although most of these features were not reproduced in the theoretical spectrum of the *E*-isomer,[21,26] the assignment has not been revised.

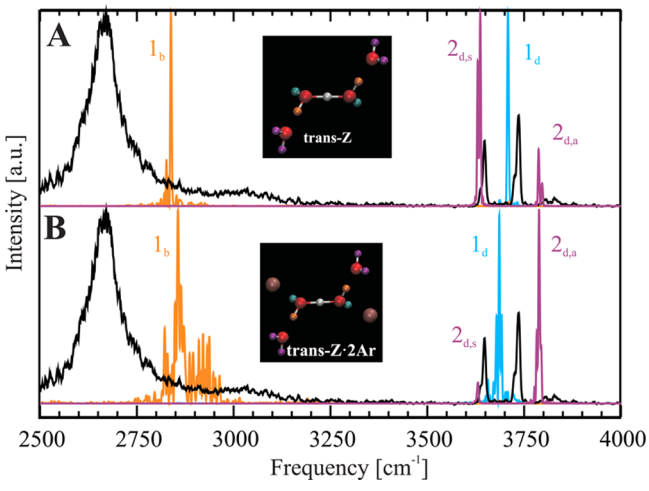

Figure 7. Comparison between the experimental IR spectrum of the Ar-tagged $H^+(H_2O)_4$ cluster[19] and the Fourier transforms of the partial VACFs for proton classes other than 0_b, in the high frequency region. Corresponding colors in the insets help identify the proton classes. (A) The trans-*Z* and (B) trans-*Z*·2Ar isomer. Note that the spectrum of each proton class is independently normalized (for visibility – to the maximal value).

Here we have performed a systematic survey of the $H^+(H_2O)_4$ cluster using an anharmonic computational method, which employs the Fourier transform of DACFs from AIMD trajectories (using the CP2K software). As a reference, we have also generated the harmonic spectra from the static, normal-mode procedure (using Gaussian 03). We have checked three isomers (*E*, cis-*Z*, and trans-*Z*), with up to three attached Ar atoms. We have also checked the effect of temperature and DC on some of these spectra.

We find that the computed spectra of the *E*-isomers are indeed in good agreement with experiment above 2000 cm^{-1} but not below. Most notably, the spectrum of the *E*·1Ar isomer is in best agreement with the dominant experimental peak at 2665 cm^{-1}, which arises from the OH stretch within the positively charged hydronium core. However, the observed peaks below 2000 cm^{-1} cannot be reproduced by any type of calculation for the *E*-isomer, irrespective of added Ar atoms, temperature variations, or DC. In contrast, we find that the linear, trans-*Z* isomer agrees with experiment in this spectral region, irrespective of Ar, DC, or temperature effects.

In the protonated dimer, the most intense peak is the shared proton mode at 1050 cm^{-1}. It was noted, however, that for less symmetric *Z*-cations it loses intensity relative to the 1750 cm^{-1} band, which becomes the dominant PTM in liquid water.[12] The $H^+(H_2O)_4$ cluster shows a characteristic band near 1050 cm^{-1}, which is indeed a shared-proton band (Figure 5A). The fact that it is less intense than the 1750 cm^{-1} band is in line with the asymmetry of the $H_5O_2^+$ core in the trans-*Z* cation.

Hence, in spite of the *E*-cluster being lowest in energy, it cannot explain the measured vibrational predissociation spectrum. The $H^+(H_2O)_4$ cluster that is commonly perceived as "the" archetypal branched *E*-cation is a linear *Z*-isomer, or a mixture of both isomers.

It is instructive to compare these gas-phase results with protonated water clusters that are trapped in liquid-phase acetonitrile (ACN), created in acidified water/ACN mixtures. As Kalish et al. show,[50] a band at 1725 cm^{-1} persists for all clusters with two or more water molecules, suggesting that they all share a Zundel core. Possibly, then, the protonated water tetramer embedded in the ACN solution is also linear rather than branched.

The fact that a short linear protonated water wire can be identified in the gas phase is potentially of great interest. Water wires are believed to conduct protons within proteins,[51,52] in carbon nanotubes,[53] or between closely spaced proton donor and acceptor in liquid water.[54−56] For example, a four-water wire with a *Z*-core was found to be a transition state in transferring a proton between protonated and unprotonated gas-phase imidazoles.[56] Hence, the present results possibly open the road for studying short water wires in isolation in the gas phase.

ASSOCIATED CONTENT

Supporting Information

A PDF with supporting Figures S1−S32 and supporting Tables S1−S11 and movies S0−S8 as .mpg files. This material is available free of charge via the Internet at http://pubs.acs.org.

AUTHOR INFORMATION

Corresponding Author

*E-mail: agmon@fh.huji.ac.il.

Notes

The authors declare no competing financial interest.

■ ACKNOWLEDGMENTS

We are indebted to Mark A. Johnson for the experimental data. This research was supported by the Israel Science Foundation (grant number 766/12). The Fritz Haber Center is supported by the Minerva Gesellschaft für die Forschung, München, FRG.

■ REFERENCES

(1) Eigen, M. Proton Transfer, Acid-Base Catalysis, and Enzymatic Hydrolysis. *Angew. Chem., Int. Ed.* **1964**, *3*, 1−72.
(2) Huggins, M. L. Hydrogen Bridges in Ice and Liquid Water. *J. Phys. Chem.* **1936**, *40*, 723−731.
(3) Zundel, G. Hydration Structure and Intermolecular Interaction in Polyelectrolytes. *Angew. Chem., Int. Ed.* **1969**, *8*, 499−509.
(4) Giguère, P. A. Comment on "H_3O^+ and OH^-, the Real Ions in Aqueous Acids and Bases". *Chem. Phys.* **1981**, *60*, 421−423.
(5) Librovich, N. B.; Sakun, V. P.; Sokolov, N. D. Reply to Comment on "H_3O^+ and OH^-, the Real Ions in Aqueous Acids and Bases". *Chem. Phys.* **1981**, *60*, 425−426.
(6) Agmon, N. The Grotthuss Mechanism. *Chem. Phys. Lett.* **1995**, *244*, 456−462.
(7) Lapid, H.; Agmon, N.; Petersen, M. K.; Voth, G. A. A Bond-Order Analysis of the Mechanism for Hydrated Proton Mobility in Liquid Water. *J. Chem. Phys.* **2005**, *122*, 014506.
(8) Markovitch, O.; Chen, H.; Izvekov, S.; Paesani, F.; Voth, G. A.; Agmon, N. Special Pair Dance and Partner Selection: Elementary Steps in Proton Transport in Liquid Water. *J. Phys. Chem. B* **2008**, *112*, 9456−9466.
(9) Marx, D.; Tuckerman, M. E.; Hutter, J.; Parrinello, M. The Nature of the Hydrated Excess Proton in Water. *Nature* **1999**, *397*, 601−604.
(10) Stoyanov, E. S.; Stoyanova, I. V.; Reed, C. A. The Structure of the Hydrogen Ion (H_{aq}^+) in Water. *J. Am. Chem. Soc.* **2010**, *132*, 1484−1485.
(11) Xu, J.; Zhang, Y.; Voth, G. A. Infrared Spectrum of the Hydrated Proton in Water. *J. Phys. Chem. Lett.* **2011**, *2*, 81−86.
(12) Kulig, W.; Agmon, N. A 'Clusters-In-Liquid' Method for Calculating Infrared Spectra Identifies the Proton Transfer Mode in Acidic Aqueous Solution. *Nat. Chem.* **2013**, *5*, 29−35.
(13) Yeh, L. I.; Okumura, M.; Myers, J. D.; Price, J. M.; Lee, Y. T. Vibrational Spectroscopy of the Hydrated Hydronium Cluster Ions $H_3O^+\cdot(H_2O)_n (n = 1, 2, 3)$. *J. Chem. Phys.* **1989**, *91*, 7319−7330.
(14) Okumura, M.; Yeh, L. I.; Myers, J. D.; Lee, Y. T. Infrared Spectra of the Solvated Hydronium Ion: Vibrational Predissociation Spectroscopy of Mass-Selected $H_3O^+\cdot(H_2O)_n\cdot(H_2)_m$. *J. Phys. Chem.* **1990**, *94*, 3416−3427.
(15) Jiang, J.-C.; Wang, Y.-S.; Chang, H.-C.; Lin, S. H.; Lee, Y. T.; Niedner-Schatteburg, G.; Chang, H.-C. Infrared Spectra of $H^+(H_2O)_{5-8}$ Clusters: Evidence for Symmetric Proton Hydration. *J. Am. Chem. Soc.* **2000**, *122*, 1398−1410.
(16) Asmis, K. R.; Pivonka, N. L.; Santambrogio, G.; Brümmer, M.; Kaposta, C.; Neumark, D. M.; Wöste, L. Gas-Phase Infrared Spectrum of the Protonated Water Dimer. *Science* **2003**, *299*, 1375−1377.
(17) Fridgen, T. D.; McMahon, T. B.; MacAleese, L.; Lemaire, J.; Maitre, P. Infrared Spectrum of the Protonated Water Dimer in the Gas Phase. *J. Phys. Chem. A* **2004**, *108*, 9008−9010.
(18) Diken, E. G.; Headrick, J. M.; Roscioli, J. R.; Bopp, J. C.; Johnson, M. A.; McCoy, A. B. Fundamental Excitations of the Shared Proton in the $H_3O_2^-$ and $H_5O_2^+$ Complexes. *J. Phys. Chem. A* **2005**, *109*, 1487−1490.
(19) Headrick, J. M.; Diken, E. G.; Walters, R. S.; Hammer, N. I.; Christie, R. A.; Cui, J.; Myshakin, E. M.; Duncan, M. A.; Johnson, M. A.; Jordan, K. D. Spectral Signatures of Hydrated Proton Vibrations in Water Clusters. *Science* **2005**, *308*, 1765−1769.
(20) Hammer, N. I.; Diken, E. G.; Roscioli, J. R.; Johnson, M. A.; Myshakin, E. M.; Jordan, K. D.; McCoy, A. B.; Huang, X.; Bowman, J. M.; Carter, S. The Vibrational Predissociation Spectra of the $H_5O_2^+\cdot Rg_n$ (Rg = Ar, Ne) Clusters: Correlation of the Solvent Perturbations in the Free OH and Shared Proton Transitions of the Zundel Ion. *J. Chem. Phys.* **2005**, *122*, 244301.
(21) Douberly, G. E.; Walters, R. S.; Cui, J.; Jordan, K. D.; Duncan, M. A. Infrared Spectroscopy of Small Protonated Water Clusters, $H^+(H_2O)_n$ (n = 2−5): Isomers, Argon Tagging, and Deuteration. *J. Phys. Chem. A* **2010**, *114*, 4570−4579.
(22) Olesen, S. G.; Guasco, T. L.; Roscioli, J. R.; Johnson, M. A. Tuning the Intermolecular Proton Bond in the $H_5O_2^+$ 'Zundel Ion' Scaffold. *Chem. Phys. Lett.* **2011**, *509*, 89−95.
(23) Mizuse, K.; Fujii, A. Tuning of the Internal Energy and Isomer Distribution in Small Protonated Water Clusters $H^+(H_2O)_{4-8}$: An Application of the Inert Gas Messenger Technique. *J. Phys. Chem. A* **2012**, *112*, 4868−4877.
(24) McCoy, A. B.; Guasco, T. L.; Leavitt, C. M.; Olesen, S. G.; Johnson, M. A. Vibrational Manifestations of Strong Non-Condon Effects in the $H_3O^+\cdot X_3$ (X = Ar, N_2, CH_4, H_2O) Complexes: A Possible Explanation for the Intensity in the "Association Band" in the Vibrational Spectrum of Water. *Phys. Chem. Chem. Phys.* **2012**, *14*, 7205−7214.
(25) Heine, N.; Fagiani, M. R.; Rossi, M.; Wende, T.; Berden, G.; Blum, V.; Asmis, K. R. Isomer-Selective Detection of Hydrogen-Bond Vibrations in the Protonated Water Hexamer. *J. Am. Chem. Soc.* **2013**, *135*, 8266−8273.
(26) Ojamäe, L.; Shavitt, I.; Singer, S. J. Potential Energy Surfaces and Vibrational Spectra of $H_5O_2^+$ and Larger Hydrated Proton Complexes. *Int. J. Quantum Chem.* **1995**, *S29*, 657−668.
(27) Ojamäe, L.; Shavitt, I.; Singer, S. J. Potential Models for Simulations of Solvated Proton in Water. *J. Chem. Phys.* **1998**, *109*, 5547−5564.
(28) Vendrell, O.; Gatti, F.; Meyer, H.-D. Full Dimensional (15-Dimensional) Quantum-Dynamical Simulation of the Protonated Water Dimer. II. Infrared Spectrum and Vibrational Dynamics. *J. Chem. Phys.* **2007**, *127*, 184303.
(29) Vendrell, O.; Meyer, H.-D. A Proton between Two Waters: Insight from Full-Dimensional Quantum-Dynamics Simulations of the $[H_2OHOH_2]^+$ Cluster. *Phys. Chem. Chem. Phys.* **2008**, *10*, 4692−4703.
(30) Frisch, M. J.; Trucks, G. W.; Schlegel, H. B.; Scuseria, G. E.; Robb, M. A.; Cheeseman, J. R.; Montgomery, J. A., Jr.; Vreven, T.; Kudin, K. N.; Burant, J. C.; et al. *Gaussian 03*; Gaussian, Inc.: Wallingford, CT, 2003.
(31) Park, M.; Shin, I.; Singh, N. J.; Kim, K. S. Eigen and Zundel Forms of Small Protonated Water Clusters: Structures and Infrared Spectra. *J. Phys. Chem. A* **2007**, *111*, 10692−10702.
(32) Cheng, H.-P.; Krause, J. L. The Dynamics of Proton Transfer in $H_5O_2^+$. *J. Chem. Phys.* **1997**, *107*, 8461−8468.
(33) Sauer, J.; Döbler, J. Gas-Phase Infrared Spectrum of the Protonated Water Dimer: Molecular Dynamics Simulation and Accuracy of the Potential Energy Surface. *ChemPhysChem* **2005**, *6*, 1706−1710.
(34) Devlin, J.; Severson, M.; Mohamed, F.; Sadlej, J.; Buch, V.; Parrinello, M. Experimental and Computational Study of Isotopic Effects Within the Zundel Ion. *Chem. Phys. Lett.* **2005**, *408*, 439−444.
(35) Iftimie, R.; Minary, P.; Tuckerman, M. E. *Ab initio* Molecular Dynamics: Concepts, Recent Developments, and Future Trends. *Proc. Natl. Acad. Sci. U.S.A.* **2005**, *102*, 6654−6659.
(36) Kaledin, M.; Kaledin, A. L.; Bowman, J. M. Vibrational Analysis of the $H_5O_2^+$ Infrared Spectrum Using Molecular and Driven Molecular Dynamics. *J. Phys. Chem. A* **2006**, *110*, 2933−2939.
(37) Kaledin, M.; Kaledin, A. L.; Bowman, J. M.; Ding, J.; Jordan, K. D. Calculation of the Vibrational Spectra of $H_5O_2^+$ and its Deuterium-Substituted Isotopologues by Molecular Dynamics Simulations. *J. Phys. Chem. A* **2009**, *113*, 7671−7677.
(38) Yu, H.; Cui, Q. The Vibrational Spectra of Protonated Water Clusters: A Benchmark for Self-Consistent-Charge Density-Functional Tight Binding. *J. Chem. Phys.* **2007**, *127*, 234504.

(39) Baer, M.; Marx, D.; Mathias, G. Theoretical Messenger Spectroscopy of Microsolvated Hydronium and Zundel Cations. *Angew. Chem., Int. Ed.* **2010**, *49*, 7346−7349.
(40) Baer, M.; Marx, D.; Mathias, G. Assigning Predissociation Infrared Spectra of Microsolvated Hydronium Cations $H_3O^+\cdot(H_2)_n$ (n = 0, 1, 2, 3) by Ab Initio Molecular Dynamics. *ChemPhysChem* **2011**, *12*, 1906−1915.
(41) Marx, D.; Hutter, J. *Ab Initio Molecular Dynamics: Basic Theory and Advanced Methods*; Cambridge University Press: Cambridge, U.K., 2009.
(42) VandeVondele, J.; Krack, M.; Mohamed, F.; Parrinello, M.; Chassaing, T.; Hutter, J. QUICKSTEP: Fast and Accurate Density Functional Calculations Using a Mixed Gaussian and Plane Waves Approach. *Comput. Phys. Commun.* **2005**, *167*, 103−128.
(43) Goedecker, S.; Teter, M.; Hutter, J. Separable Dual-Space Gaussian Pseudopotentials. *Phys. Rev. B* **1996**, *54*, 1703−1710.
(44) Martyna, G. J.; Tuckerman, M. E. A Reciprocal Space Based Method for Treating Long Range Interactions in Ab Initio and Force-Field-Based Calculations in Clusters. *J. Chem. Phys.* **1999**, *110*, 2810−2821.
(45) Grimme, S.; Antony, J.; Ehrlich, S.; Krieg, H. A Consistent and Accurate Ab Initio Parametrization of Density Functional Dispersion Correction (DFT-D) for the 94 Elements H-Pu. *J. Chem. Phys.* **2010**, *132*, 154104.
(46) Watkins, M.; VandeVondele, J.; Slater, B. Point Defects at the Ice (0001) Surface. *Proc. Natl. Acad. Sci. U.S.A.* **2010**, *107*, 12429−12434.
(47) Agostini, F.; Vuilleumier, R.; Ciccotti, G. Infrared Spectroscopy of Small Protonated Water Clusters at Room Temperature: An Effective Modes Analysis. *J. Chem. Phys.* **2011**, *134*, 084302.
(48) Aida, M.; Dupuis, M. IR and Raman Intensities in Vibrational Spectra from Direct Ab Initio Molecular Dynamics: D_2O as an Illustration. *J. Mol. Struct.* **2003**, *633*, 247−255.
(49) Hesske, H.; Urakawa, A.; VandeVondele, J.; Baiker, A. Insight into Fundamental, Overtone, and Combination IR Bands of Surface and Bulk $Ba(NO_3)_2$ by Ab Initio Molecular Dynamics. *J. Phys. Chem. C* **2010**, *114*, 15042−15048.
(50) Kalish, N. B.-M.; Shandalov, E.; Kharlanov, V.; Pines, D.; Pines, E. Apparent Stoichiometry of Water in Proton Hydration and Proton Dehydration Reactions in CH_3CN/H_2O Solutions. *J. Phys. Chem. A* **2011**, *115*, 4063−4075.
(51) Garczarek, F.; Gerwert, K. Functional Waters in Intraprotein Proton Transfer Monitored by FTIR Difference Spectroscopy. *Nature* **2006**, *439*, 109−112.
(52) Shinobu, A.; Agmon, N.; Schierbeek, A. J.; Palm, G. Visualizing Proton Antenna in a High Resolution Green Fluorescent Protein Structure. *J. Am. Chem. Soc.* **2010**, *132*, 11093−11102.
(53) Cao, Z.; Peng, Y.; Yan, T.; Li, S.; Li, A.; Voth, G. A. Mechanism of Fast Proton Transport along One-Dimensional Water Chains Confined in Carbon Nanotubes. *J. Am. Chem. Soc.* **2010**, *132*, 11395−11397.
(54) Cox, M. J.; Timmer, R. L. A.; Bakker, H. J.; Park, S.; Agmon, N. Distance-Dependent Proton Transfer along Water Wires Connecting Acid-Base Pairs. *J. Phys. Chem. A* **2009**, *113*, 6599−6606.
(55) Hassanali, A.; Prakash, M. K.; Eshet, H.; Parrinello, M. On the Recombination of Hydronium and Hydroxide Ions in Water. *Proc. Natl. Acad. Sci. U.S.A.* **2011**, *108*, 20410−20415.
(56) Kaila, V. R. I.; Hummer, G. Energetics and Dynamics of Proton Transfer Reactions along Short Water Wires. *Phys. Chem. Chem. Phys.* **2011**, *13*, 13207−13215.